Environ Earth Sci (2012) 67:273–283
DOI 10.1007/s12665-011-1506-x

ORIGINAL ARTICLE

Karstological study of the new Kunming airport building area (Yunnan, China)

Martin Knez · Janja Kogovšek · Hong Liu · Janez Mulec · Metka Petrič · Nataša Ravbar · Tadej Slabe

Received: 7 December 2010 / Accepted: 13 December 2011 / Published online: 23 December 2011

Abstract In Kunming area (6.8 mio population), two big interventions are in progress: construction of a new airport, the 23 km^2 area of which will extend across karst terrain northeast of the city, and extensive uptake of water from karst aquifers for drinking and agricultural use. In the study, an interdisciplinary approach was utilized to demonstrate the need for holistic karstology studies prior to performing extensive interferences in the karst environment. This study included survey of surface karst features and microscopic analyses of rock samples in the area of the new airport location, accompanied by hydrogeological studies and microbiological analyses of two karst drinking water sources in its vicinity (Qinglongdong, Huanglongdong). Results showed the specific characteristics of the subsoil stone forest that indicated a high level of karstification. The direction and characteristics of groundwater flow from the sinking Qiaotou Stream at the margin of the new airport area toward the Huanglongdong Spring were defined with a single tracer test. Additional information about hydrogeological characteristics of the karst aquifer was obtained by individual measurements of physical and chemical parameters of the springs and sinking stream. Selected chemical and bacteriological parameters showed substantial pollution of both springs due to various types of human activities in the catchments. The results of the study pointed to the necessity of taking immediate measures for the springs' protection and showed the importance of interdisciplinary research when planning anthropogenic activities in the karst.

Keywords Building on karst · Surface landforms · Karst water sources · Water quality · Tracer test · China

M. Knez · J. Kogovšek · J. Mulec · M. Petrič (✉) · N. Ravbar · T. Slabe
Karst Research Institute ZRC SAZU, Titov trg 2, 6230 Postojna, Slovenia
e-mail: petric@zrc-sazu.si

H. Liu
Yunnan Institute of Geography, Yunnan University, Xuefu Rd. 20, 650223 Kunming, China

Introduction

The exceptional and diverse features of the Yunnan karst (SW China), from the tropical cone karst in the south and the stone forests in the center to the mountain karst and high plateau karst of Tibet in the north, offer a revelation of the basic characteristics of how karst is formed. The relatively dense settlement of the region and urban expansion, growing industry and infrastructure development, intensified agriculture, growing tourism and the corresponding great need for clean water offer opportunities for research and even demand that karstologists study the modern human impact on this vulnerable karst region (Chen et al. 1998; Guo and Jiang 2010; Guo et al. 2010; Jiang et al. 2008, 2009; Knez et al. 2009, 2010a, 2010b; Kogovšek 2010; Lu 2006; Shi et al. 2009).

Kunming, the capital city of Yunnan, experiences such pressures, which have already taken its toll on the environment and water supply resources; therefore, the implementation of sustainable planning and management practices is necessary. The city covers a total land area of 21,111 km^2 and has at present a total population of 6.8 million. It serves as a gateway to neighboring countries, Vietnam, Laos and Myanmar, and its development strategy is centered on building itself up as a regional and international commercial and tourism center. Because the location of the currently operating airport does not allow

for further expansion, a new airport is being built about 21 km northeast of the city and is planned to be the air logistics center to link with south and southeast Asia. The first phase of the project was planned for the 5 year period between 2006 and 2011, and the project should be finished and the airport built on an area of almost 23 km^2 by 2020.

This very extensive project will have numerous consequences for its entire area of influence, which is predominantly karstic. In the framework of the bilateral Slovene–Chinese project titled *The impact of airport construction on karst aquifer behaviour and water quality—case study of Qinglongdong spring catchment, Kunming, China*, a number of studies on the geological, geomorphological and hydrogeological characteristics of the karst part of the area have been conducted since 2006. Field work in the following years when the earthworks started allowed us to monitor the changes in the open surfaces and study surface karst forms that revealed the specific characteristics of the subsoil stone forest in this area.

Karst waters were monitored at selected points in ponors and springs. Physical properties were measured and samples collected for chemical and bacteriological analysis. Based on the collected data, certain hydrogeological problems were identified and studied in detail. Special interest was aroused by the Huanglongdong and Qinglongdong springs located southwest of the location of the new airport (Fig. 1). In the absence of any better solutions, these two springs are potential water supply sources even though they are already quite polluted due to various sources of pollution in their catchment areas. It is interesting that despite a distance of only 500 m between them, they display significant differences in their physical and chemical characteristics. Further studies were therefore oriented toward establishing the differences between the catchment areas of the two springs and the characteristics of flow inside the catchment areas, an important basis for assessing the potential impact of the construction of the new airport and planning their protection.

Basic research was augmented by a tracer test. Due to technical problems, the originally planned tracing of a sinking stream in the central construction area of the new airport was rescheduled for a later period. In May 2009, a tracer test on a sinking stream 1 km north of the Huanglongdong and Qinglongdong springs was carried out. This paper summarizes the results of the research conducted so far.

Study site

Basic geological and hydrogeological characteristics from existing geological maps of the study area were summarized and augmented with additional field surveys.

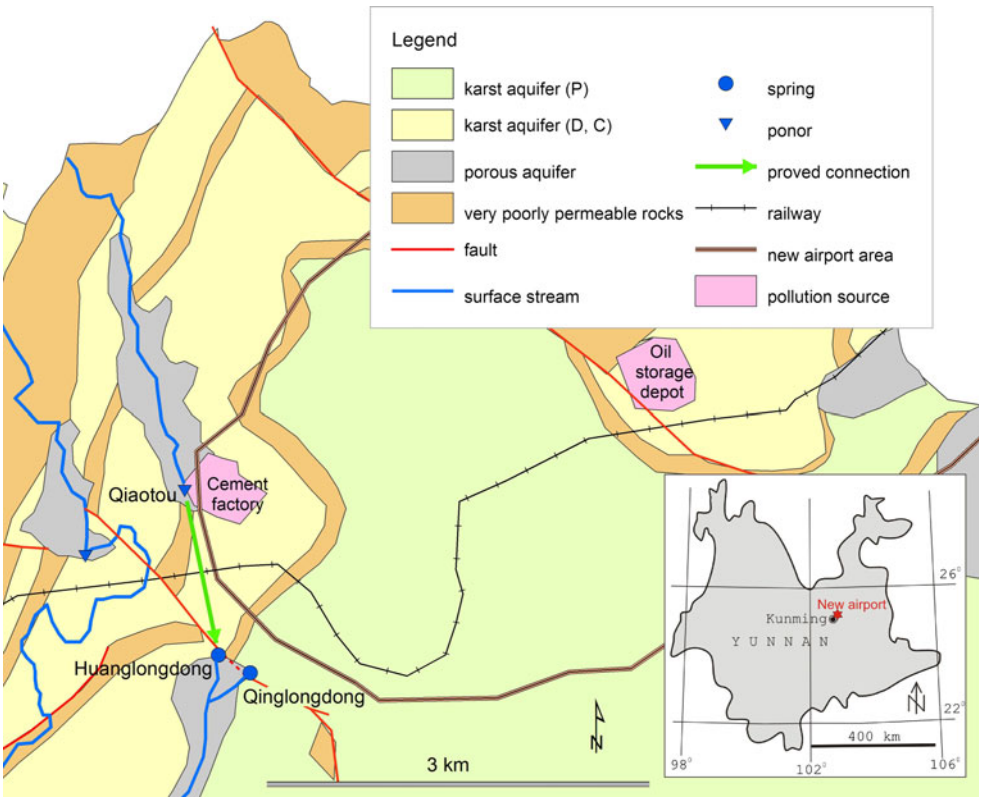

Fig. 1 Hydrogeological map of the study area

Carbonate rock of Cambrian to Permian age dominates in the area of the new airport and the Huanglongdong and Qinglongdong springs (Fig. 1). It is composed largely of dolomite with slightly more limestone only in the Lower Permian beds. These beds, which outcrop in the southeastern part of the study area, display the most karstification with developed characteristic karst forms. Hydrogeological barriers between beds of karst rock are composed of very poorly permeable Cambrian, Carboniferous and Permian clastic rocks. Quaternary alluvial sediments are deposited along surface water courses. Undulating karst landscape with the altitude differences of up to 50 m traverses from karst hills to shallow depressions and dolines. The area is used as agricultural land with orchards or corn fields in the karst areas, and vegetable and rice fields on Quaternary alluvial sediments.

The Qinglongdong and Huanglongdong springs are located at the contact between the karst aquifer in carbonate rock and poorly permeable alluvial sediment. The area between them is cut by a subvertical fault running northwest–southeast and a thinner belt of very poorly permeable Permian clastic rocks. This belt continues in a northerly direction and presumably plays the role of a hydrological barrier separating the catchment areas of the two springs. Inside the catchment areas, there are several sinking streams that collect water from different areas, and the direction of their underground courses has not been reliably proven. The Qiaotou Ponor, which lies about 1 km north of the springs, was included in the study.

The Qinglongdong Spring (Fig. 2a) was part of the Kunming region water supply system, but pumping stopped in 2002 due to pesticide pollution. In 2005, pumping resumed due to a shortage of suitable water sources. The Huanglongdong Spring (Fig. 2b) has also been captured for water supply purposes. However, no appropriate measures for the protection of their catchment areas have been enacted. According to the hydrogeological map, the springs are supplied by the aquifer to the north and east of the springs, but there have been no more detailed studies. Well-developed karst forms (sinkholes, karren, ponors, etc.) indicate good karstification of the area. Despite the relative thickness (>1 m) of the soil layer, the infiltration at the mentioned points is rapid and followed by underground flow through well-developed karst channels and fissures toward the springs through which the water returns to the surface at the contact with poorly permeable rock. The thickness of the vadose zone does not exceed 100 m and usually measures from 40–50 m.

The mean annual discharge of the Qinglongdong Spring is 473 l/s, minimal discharges total a few liters per second, and maximum discharges can reach up to 3 m^3/s or more. In the Kunming area, the mean annual air temperature for a 30 year period is 14.5°C and the mean annual precipitation is 1,035 mm (Zhang et al. 2005). According to the Turc equation (Shaw 1994), the mean annual evapotranspiration can be estimated at about 650 mm. Taking this data and the mean annual discharge of the Qinglongdong Spring into consideration, the minimum extent of the catchment area can be estimated at about 39 km^2.

Karst surface dissected into subsoil stone forest

The surface of the hilly area was dissected by low, up to 1 m high or sometimes slightly higher, and relatively sparse karren with pointed and stumpy rock peaks. They were separated by larger or smaller patches of sediment covered by soil and shrubs or trees. The earthworks revealed a subsoil stone forest (Fig. 3) covering almost the entire area of carbonate rock that boasts unique form characteristics, dictated largely by the composition of the rock. The karren that dissected the surface was the top of the subsoil stone forest.

The rock is fractured by subvertical faults, 5–10 m apart. The faults generally run in the north–south and east–west directions (Fig. 4). Karst processes have denuded the rock laterally along the faults many meters in width and up

Fig. 2 Qinglongdong (**a**) and Huanglongdong (**b**) springs

Fig. 3 Subsoil stone forest

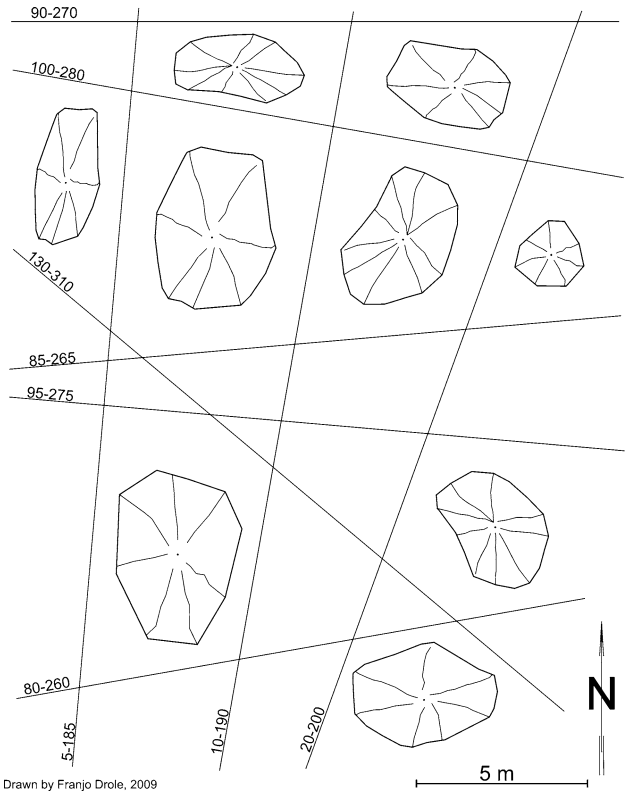

Fig. 4 Ground plan of tops of stone pillars with drawn subvertical faults

to 10 m deep. Larger rock masses or stone pillars remain today only where the fault network is less dense.

The dissection of the rock surface, dictated by the composition of rock with relatively large dolomite lenses, gave a special stamp to the subsoil stone forest (Fig. 5a). The lenses are about 20 cm in diameter and up to several cubic decimeters in volume. The textural characteristics of light brown to light gray solid and homogenous limestone dominate the entire area.

The rocky surface of the pillars is defined by the characteristics of the rock's composition and the conditions of its formation. The frequency of dolomite lenses varies. In places where their frequency in the rock is high, they project from the walls one next to another as a rule. Where there are only individual dolomite lenses in the rock, single semicircular recesses occur frequently. The surface of rock with no lenses is smooth below the ground, while on the surface it is dissected by traces of rainwater and water creeping down the walls.

Due to their convex shape, greater roughness and consequently heavier lichen cover, dolomite lenses on the surface of the rock are a dark gray in color and are visible on the surface of the rock as dark gray to black patches on a lighter colored base (Fig. 5a). For the most part, the percentage of undolomitized limestone surface is only a little less than the percentage of dolomitized sections. In spite of this, relative to all the studied rock columns, the proportion of dolomitized sections is not equally distributed and tends to change laterally, though never completely disappearing in the studied area. Rock with such properties limits the development of smaller subsoil rock forms as well as rock forms carved by rainwater.

Stratification in the solid and homogenous rock is almost never observed, but in individual places largely horizontal contacts between rock segments can be seen. Bearing this in mind, rock samples were collected in the vertical direction from one of the pillars.

An important general property of the rock is primarily strong diagenetic change in the limestone: recrystallization, dolomitization and in certain places considerable secondary porosity and a high percentage of carbonate (Table 1).

Studies of microscopic thin sections showed that in the lower section of the karren, some 10 m below the recent surface, the original limestone is late diagenetically dolomitized. In the wackestone to packstone type of limestone, poorly identifiable fragments of fossil remains can be observed, parts of which have often been microscopically displaced along tiny fissures. Pellets and other lithic grains occur frequently. The rock is crisscrossed by tiny calcite veins running in various directions with cross sections measuring from 0.5 to 2 mm. Calcite fills mostly spherical fenestrae 2–10 mm in size.

In some places, the frequency and size of dolomitized sections change laterally as well as vertically. Due to the mostly idiomorphic grains of dolomite around 0.25 mm in diameter, the rock can be labeled the grainstone type of dolosparite. The grains of dolomite are poorly cemented, but to a great extent the grains remain in place on the surface of the rock in fissures widened by corrosion and filled by sediment. Secondary intergranular porosity

Fig. 5 In some places, lenses of dolomitized limestone (*dark gray*) measure up to several dm^3 in volume (width of view is 25 cm) (**a**). Weathered rock is more than 5 cm thick in places (width of view is 20 cm) (**b**)

Table 1 Results of calcimetric analyses of rock samples

Rock sample	CaO	MgO	Dolomite	Total carbonate (%)	Calcite	CaO/MgO	Insoluble residue
10 m below surface	47.94	7.18	32.82	100	67.18	6.67	0.00
10 m below surface	46.43	8.16	37.81	100	62.19	5.68	0.00
8 m below surface	54.23	1.81	8.29	100	91.71	29.96	0.00
8 m below surface	54.22	1.57	7.19	100	92.81	34.53	0.00
5 m below surface	55.46	0.80	3.69	100	96.31	69.32	0.00
4 m below surface	55.97	0.52	4.79	100	55.21	107	0.00
2 m below surface	55.40	0.48	2.21	99.92	97.71	115	0.00
Surface	56.08	0.08	0.36	100	99.64	7.01	0.00
Dolomite lens	37.29	15.76	72.10	99.51	27.41	2.05	0.00
Weathered rock surface	41.38	12.86	58.82	100	41.18	3.22	0.00

changes laterally, generally estimated at around 5–10%. The possibility of subsoil weathering of rock is great, primarily due to the considerable porosity of the rock and the poorly cemented dolomite crystals. On the lowest sections of the stone pillars where sediment has been recently removed, the thickness of weathered rock can exceed 5 cm (Fig. 5b). Dolomite lenses protrude here most from the surface of the rock, and the characteristic boxwork pattern can be observed on the surface.

The ratio between basic non-dolomitized rock and dolomite lenses does not change substantially in the central part of the karren. However, numerous completely regular idiomorphic crystals of dolomite whose sharp edges indent in various clasts (e.g., foraminifers up to 5 mm in size) appear in the limestone. The ratio of calcite to late diagenetic idiomorphic dolomite is 1:1. Recrystallized corals as well as numerous fragmented foraminifers are frequently found in this section. The rock is crisscrossed by microtectonic fissures filled with calcite. In some places, calcite veins are slightly dolomitized. Plasticlasts up to 1 cm in size are also encountered on rare occasion in the rock.

The rock forming the tops of the rock pillars also changes strongly laterally. In part of the rock, calcite and dolomite crystals (around 0.25 mm in diameter) appear in the same proportion. In another part, the pelmicrosparite type of limestone with numerous fenestrae filled with calcite sparite and individual calcite veins up to 1 mm thick appears. The limestone contains numerous fragments of unidentifiable foraminifers and other mollusks. Where dolomite crystal grains and calcite alternate in more or less equal proportions, the fossil remains are no longer visible due to recrystallization. Tiny fissures up to 1 mm thick are filled with sparite cement. Grains of dolomite in dolomite lenses are poorly cemented and are therefore easily washed from the rock surface by various erosion processes.

Relatively large stone pillars dominate in the subsoil stone forest. Their lower sections are five or more meters in diameter. As a rule, the pillars end in a number of conical peaks, and some pillars have wide tops dissected below the ground. The pillars measure up to 10 m in height. The larger, often elliptical cross sections of the pillars and differences in their size reflect the sparser and unsymmetrical network of fissures that vertically cut the carbonate

rock and widen below the ground between the pillars (Fig. 4).

The rock relief (Slabe 1998) clearly shows the subsoil formation (Slabe 2005) of the stone pillars below the soil and sediment that cover the carbonate rock and the transformation of the denuded tops. The rock surface is quite unique, dictated largely by the specific rock composition. The most distinct rock forms are subsoil channels (Slabe and Liu 2009) that dissect the walls and tops of the pillars. The vertical channels frequently have extensive funnel-like mouths at the top and measure 1 m or more in diameter; however, smaller and more or less horizontal channels wind only between the peaks. Subsoil cups also formed in the latter. From the surface, water creeps through the channels along the contact of sediment and soil with the rock. The funnel-like mouths of subsoil channels in connected semicircular notches wind and dissect extensive more or less horizontal tops of pillars or wind between their conical peaks. Smaller subsoil shafts up to 20 cm in size are of similar origin and vertically hollow as the pillars and smaller tubes of the same size that crisscross them in various directions, which in some places indicate porous rock. Shafts and cavities form at the contact with the sediment that fills them. The walls of individual pillars are undercut or dissected by horizontal notches, the consequence of accelerated corrosion caused by stagnant percolating water at the contact with sediment that is poorly permeable in some places. Subsoil cups and only a few slightly slanting channels formed on the wider tops. Soil and sediment only cover the rock in some places, which below them dissolves to form cups and channels.

Characteristic rock relief dissects the tops of pillars that were denuded and exposed to rain. The rock forms include rain flutes, rain pits, solution pans and scallops that formed due to the creeping of water down the overhanging surface of the wall. The rain flutes (Slabe 2005) could only form on limestone rock between nodules of dolomite. Solution pans developed as a rule from subsoil cups when the tops of the pillars were denuded. Their dissected and jagged form was dictated by the composition of the rock as the rain transformed denuded subsoil rock forms. The walls of funnel-like mouths of subsoil channels are dissected by flutes. Rain pits are found on horizontal flat surfaces of the tops; conical tops are the consequence of quarrying activity. Below the moss layer, biocorrosion sculpts smaller pits and channels.

Relative to conditions, the formation of the rock surface can be divided into three characteristic parts. Nodules on the surface exposed mostly to rain and corrosion are relatively angular, dissected by tiny notches and rain pits that formed along tiny fissures due to the uneven composition of the rock. On larger limestone surfaces, flutes formed between the nodules on slanted rock and solution pans occurred on horizontal rock. Their edges are dissected and jagged because their walls are often dolomite nodules. The surface of rock surrounded by soil is similar since immediately below the ground where dissolution is most pronounced due to organic matter in the soil, water erodes grains of dolomite rock at a faster rate along a permeable contact. The nodules protrude semispherically, most distinctly from walls that are deeper below the surface. The contact between the rock and sediment is poorly permeable and therefore the saturated water drains away at a slower rate. This is also evident in the weathered layer of the rock. Individual sparry calcite protrudes from all surfaces.

Below the stone forest, there is a well-developed network of caves through which water courses flow and carry away sediment washed from the surface by rainwater, enabling their growth despite the poor permeability of the contact between the rock and the sediment.

Measurements of physical and chemical parameters and bacterial indicators

Methods

A datalogger with probes for the continuous measurement of water level, temperature (T), electrical conductivity (EC) and pH at 15 min intervals was installed at the Qinglongdong Spring in February 2007 and data were collected until September 2007. The discharges of both springs were measured in July 2008 and May 2009 with an OTT C20 Current Meter, and of the Qiaotou Ponor in May 2008. At the time of other samplings, the discharge was estimated. It must be noted that only the discharge at the channel was measured or estimated because data on the amount pumped for the supply of the population with water were not available at every monitoring.

Between 2006 and 2009 in the period from May to August, the water was sampled for physical and chemical analyses, five times at the Qinglongdong and Huanglongdong springs and three times at the Qiaotou Ponor. Each time, T and EC were measured. In 2006 and 2009, the WTW MultiLine P4 was used, and in 2007 and 2008 the WTW 330i conductometer. The two instruments were intercalibrated. Analyses on the content of nitrates, *o*-phosphates, and ammonium using the corresponding Visicolor-ECO colorimetric tests were done in field laboratories. Total hardness (Ca + Mg) and calcium content (Ca) were determined using the standard titrimetric method (Greenberg et al. 1992).

Environmental microbiology uses indicator organisms as a criterion of water quality and as a warning of possible contamination. The following microbial groups are used to determine the microbiological safety of water: total

coliforms (these bacteria are classically used as indicators of fecal contamination, although some members of this group can originate from nonenteric environments), fecal coliforms (thermotolerant coliforms, particularly *Escherichia coli*), fecal streptococci and enterococci, sulfite-reducing clostridia, *Pseudomonas* spp. and heterotrophic plate counts that indicate the overall microbiological status of the system (Toranzos and McFeters 1997). A high number of fecal coliforms (>200 colonies/100 ml) in a river or stream indicate a high probability of the presence of pathogenic microbes.

For bacteriological analysis, water samples from the Qinglongdong and Huanglongdong springs and the Qiaotou Ponor were collected in 50 ml sterile test tubes (6 May 2009; dry, sunny weather). Since the tested water appeared clear at the springs and the ponor, membrane filtration was not applied. Ridacount medium plates (R-biopharm, Germany) were used for quantitative microbial detection (Mulec et al. 2012). Ridacount plates are made of a base film coated with a dry culture medium and covered with a fabric that allows perfect absorption of an applied sample solution. At the site 1 ml samples of water were directly applied onto the plates to determine the total number of aerobic heterotrophic bacteria (Ridacount Total) and coliform bacteria (Ridacount Coliform). The Ridacount Coliform test is based on the β-galacotosidase activity of coliform bacteria. The plates were incubated 24 h at 35°C for coliforms and 48 h at 35°C for total bacterial heterotrophic counts (R-Biopharm). After the incubation was completed, bacterial colonies were enumerated and expressed as CFU (colony-forming units) per ml.

Results

Water pumping has a characteristic and decisive impact on the measured levels of water in the Qinglongdong Spring. No data on the time distribution and volume of pumping are available, so a comparison of the measured levels with hydrological conditions is therefore not possible. During the operation of the datalogger between February and September 2007, the water temperature was very constant, oscillating between 16.7°C and 16.9°C. Similarly, pH values varied between 6.9 and 7.3. EC values oscillated between 369 and 480 μS/cm, depending on the hydrological conditions.

During manual sampling in the 2006–2009 period (Table 2), the measured temperatures of the Quinglongdong Spring oscillated minimally (16.6–16.8°C), while the Hunglongdong Spring oscillated more distinctly (16.1–19.5°C). The EC of the Qinglongdong Spring oscillated between 404 and 483 μS/cm, while the Huanglongdong Spring oscillated between 329 and 519 μS/cm. The lowest values were recorded during the highest discharges. The larger oscillations of T and EC in the Huanglongdong Spring compared to the Qinglongdong Spring can be explained by the inflow of surface water.

During the high water level in July 2008, the Ca/Mg ratio of the Hunglongdong Spring was 1 or 1.5 (Fig. 6), and the ratio of the water at the Qiaotou Ponor was the same. This indicates a possible connection between the ponor and this spring, because the Qinglongdong Spring had higher ratios: 3.8 at low discharge and 6 at high discharge in July 2008. The ponor, and even more so the two springs, displayed increased content of nitrates (from 3 to 70 mg of NO_3^-/l) and *o*-phosphates (up to 0.7 mg of PO_4^{3-}/l), and the Huanglongdong Spring's concentrations of chlorides and sulfates were even higher. It is obvious that the underground flow from the ponor to this spring receives additional pollution from the vadose zone depending on the hydrological conditions.

For assessing the quality of drinking water, several ISO methods are applied to detect crucial microbiological

Table 2 Measurements of physical parameters of manually collected samples in the 2006–2009 period

Place	Date	Q (l/s)	T (°C)	EC (μs/cm)
Qiaotou sinking stream	July 4, 2008		17.3	303
	May 6, 2009	16	21.6	414
	August 16, 2009	200 (est.)	20.7	364
Qinglongdong Spring	June 13, 2006	Low (est.)	16.6	463
	May 24, 2007		16.8	433
	July 4, 2008	2,100	16.6	404
	May 6, 2009	91	16.7	432
	August 16, 2009	250 (est.)	16.8	483
Huanglongdong Spring	June 13, 2006	200 (est.)	18.7	472
	May 24, 2007	200 (est.)	17.4	480
	July 4, 2008	1,800	17.2	329
	May 6, 2009	30 (est.)	16.1	519
	August 16, 2009	1,000 (est.)	19.5	718

est. estimated

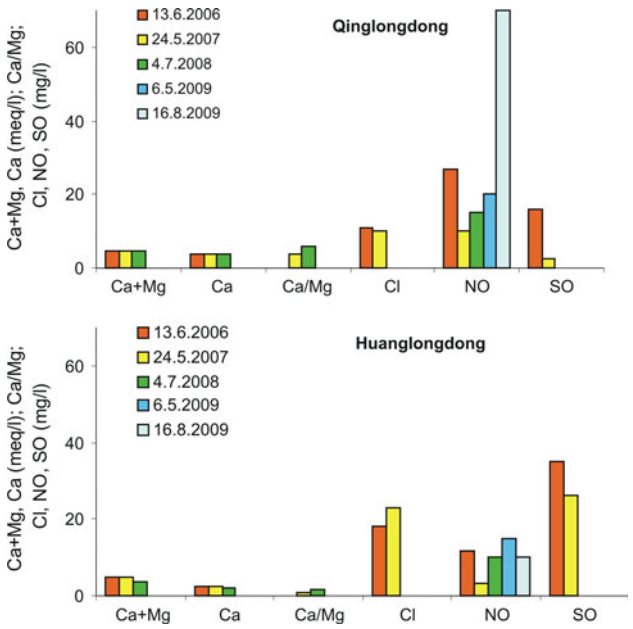

Fig. 6 Chemical parameters of manually taken samples: Ca + Mg-total hardness, *Ca* calcium, *Cl* chlorides, *NO* nitrates, *SO* sulfates

parameters (*Escherichia coli*, coliform bacteria, enterococci, *Clostridium perfringens*, number of colonies at 22°C, total number of colonies at 37°C). Ridacount test plates were successfully used to determine the water quality of the Qinglongdong and Huanglongdong springs and the Qiaotou Ponor and proved to be a reliable field test to quickly determine the possible existence of water contamination dangerous to public health. To determine water quality, we measured total bacterial count and the number of coliforms (Fig. 7). Based on ISO standards for drinking water, the number of coliforms must not exceed 0 CFU in a 100 ml sample of water (SIST EN ISO 9308-1) and the total number of mesophilic bacteria at 37°C must be under 100 CFU per ml (SIST EN ISO 6222). The total heterotrophic bacterial count takes into consideration the enumeration of all aerobic bacteria capable of growing on nutrient-rich media. In the case of the water sample from the Qinglongdong Spring, the lower number of the total bacterial count (22 CFU/ml) compared to the coliform count (31 CFU/ml) is attributed to the uneven distribution of water samples on the Ridacount Total test plates (Table 3). None of the water from any of the tested sites matched the ISO criteria, and it is not suitable for direct public consumption without downstream processing to remove bacteria. This issue is even more urgent, since coliforms have been shown able to grow in potable water distribution systems as a result of bacterial biofilms on pipe surfaces, and consequently the total number of coliform bacteria reaching the end-users can be even higher (Toranzos and McFeters 1997).

Tracer test

Methods

A tracer test was employed to determine where the water from the Qiaotou Ponor flows and to assess the characteristics of this underground flow. At 18:00 h on 7 May 2009, when its discharge was 16 l/s at a low water level, 50 g of uranine was injected at the ponor (Fig. 8). Before the injection and 30 days after it, samples were taken at the Qinglongdong and Huanglongdong springs. During the injection, the discharge at the Qinglongdong Spring was around 90 l/s and about three times lower at the Huanglongdong Spring. Hydrological conditions remained stable until 14 May 2009, when heavier rains started. The samples were analyzed for the presence of uranine (E_{ex} = 491 nm, E_{em} = 512 nm; detection limit 0.005 mg/m^3) at the Karst

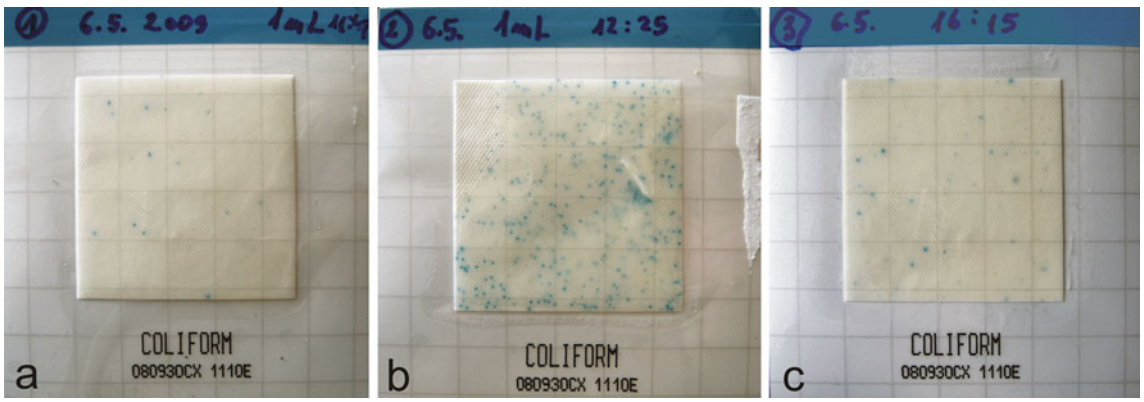

Fig. 7 Counts of coliform bacteria based on β-galacotosidase activity used for determining water quality for Qinglongdong Spring (**a**), Huanglongdong Spring (**b**) and Qiaotou Ponor (**c**)

Table 3 Water quality assessment based on selected bacterial indicator groups and expressed as colony-forming units (CFU) per ml

Site	Bacterial indicator group	
	Total bacterial count (CFU/ml)	Coliform count (CFU/ml)
Qinglongdong Spring	22[a]	31
Huanglongdong Spring	800	250
Qiaotou sinking stream	300	41

[a] Uneven distribution of sample

Fig. 8 Injection of uranine in Qiaotou Ponor

Research Institute in Postojna, Slovenia, using a Perkin Elmer LS 30 fluorescent spectrometer.

Results

In the existing hydrological conditions when the discharge was low, the first traces of the injected uranine were observed at the Huanglongdong Spring at 20:00 h on 10 May 2009, 3 days and 2 h after the injection (Fig. 9). Over the next 26 h, the concentration of uranine increased to its maximum value of 2.9 mg/m^3 and then decreased, falling below the detection limit on 16 May 2009. In Qinglongdong, no tracer was detected. During the period of decreasing, the concentration oscillated twice (in the early morning hours on 12 and 13 May), even though there was no rain. The cause might have been a changed pumping regime, but no measurements of the discharge were made at the time that might explain the rises in the concentration. The first rain after the injection fell on 14 May, when very low concentrations of the tracer had already been observed at the spring. No changes in uranine concentration following this precipitation event and increased discharge were observed. Also in the following period until 26 May 2009, when the estimated value of the discharge of the spring was 2.5 times higher than at the injection, the concentration of the tracer recorded no rises and remained below the detection limit until the end of sampling. This indicates that the majority of the tracer was transferred during the observed tracer wave. Given the surface distance between the ponor and the spring (1,250 m), the apparent maximum velocity at low water levels is 17 m/h, and the dominant velocity is 12.5 m/h. At the Qinglongdong Spring, the concentration of uranine oscillated around the detection limit, and individual higher values were only recorded twice (0.03 and 0.02 mg/m^3). These minor oscillations probably reflect natural fluorescence oscillations and lead to the conclusion that in the existing hydrological conditions, there is no water connection between the Qiaotou Ponor and the Qinglongdong Spring.

Discussion

Based on individual measurements of physical and chemical parameters taken under various hydrological conditions and a tracer test, the characteristics of the recharge areas of the Qinglongdong and Huanglongdong springs were assessed. They are located inside the area composed of carbonate rock of Cambrian to Permian age. Although the distance between the springs is only 500 m, they display significant differences in their characteristics.

The possibility of the existence of two separated recharge areas is indicated by the geological structure. The Devonian and Carboniferous carbonate rock in the northwestern part of the study area is composed largely of dolomite, while the Lower Permian carbonate rock in the

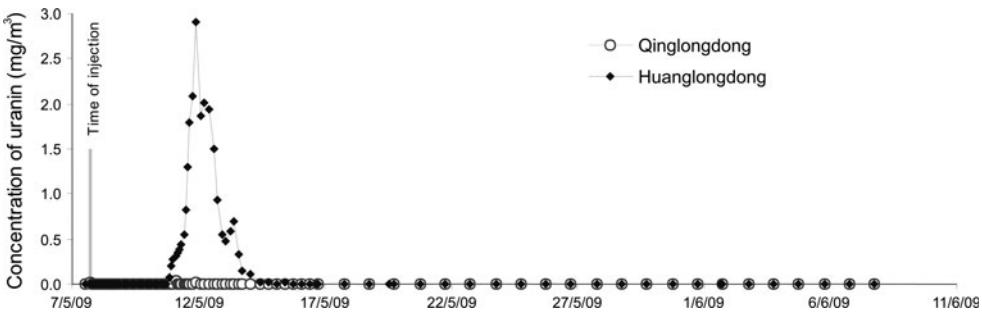

Fig. 9 Tracer breakthrough curves for Huanglongdong and Qinglongdong springs

southeastern part has more limestone. These lithological differences are reflected in the chemical composition of the two springs, especially in the Ca/Mg ratio. Lower Ca/Mg values of the Huanglongdong Spring (1–1.5) indicate recharge from a dolomite catchment. It is possible to infer that the Huanglongdong Spring is mainly recharged from the karst aquifer in the northwestern part, which is slightly less permeable and composed largely of dolomite, and the Qinglongdong Spring from the karst aquifer in the southeastern part with larger share of limestone and higher permeability. An intermediate, narrow belt of very poorly permeable Permian clastic rocks acts as a hydrogeological barrier. By the tracer test and a similar chemical composition proved underground water connection between the Qiaotou Ponor and the Huanglongdong Spring and the absence of injected tracer in the Qinglongdong Spring support the above stated conclusion.

The ratio between the minimum and maximum discharge of the Qinglongdong Spring is at least 1:300, which is characteristic for the karst type of springs with fast groundwater flow through well-developed karst channels in its catchment. No long-term data on discharge of the Huanglongdong Spring are available. However, the existing occasional measurements show similar characteristics. Also, the shape of the tracer breakthrough curve indicates a fast flow through karst channels from the Qiaotou Ponor to the Huanglongdong Spring. Even though no precipitation event occurred in the first week of sampling, a continuous and uniformly shaped breakthrough curve with a peak 4 days after the injection was formed. A dominant role of groundwater flow through karst channels was additionally confirmed by the fact that no increases of tracer concentrations were detected after some intensive precipitation events later in the period of sampling. Based on the test results, the apparent maximum velocity at low water levels of 17 m/h, and the dominant velocity of 12.5 m/h were calculated. Considering the hydrogeological characteristics of the study area, it seems possible that the flow velocities in the catchment of the Qinglongdong Spring are higher than in the catchment of the Huanglongdong Spring.

The calculated velocities are more than two times smaller than for the underground flow in the karst aquifer of well-permeable Carboniferous and Permian limestone in the Tianshengan area (region of Lunan, Yunnan), which we traced at low water levels in 1998 (Kogovšek and Liu 1999). As in this area the apparent velocities were more than three times higher during the tracer test at high water levels (Kogovšek 2010), also the velocities of flow in both parts of the study area are probably considerably higher at high water levels.

Different types of recharge are characteristic for the two parts of the study area. Significantly higher oscillations of physical parameters in the Huanglongdong Spring (T oscillates for 2.3°C and EC for 190 μS/cm) than in the Qinglongdong Spring (T oscillates for 0.2°C and EC for 79 μS/cm) indicate an influence of allogenic recharge with sinking streams in the catchment of the Huanglongdong Spring. A direct connection between the Qiaotou Ponor and the spring has already been indicated by the comparison of chemical parameters, and then further confirmed by the tracer test. It is however possible that this spring is additionally recharged from some other sinking streams in the vicinity. In the Qinglongdong Spring, no tracer was detected and according to the known characteristics also the connection with some other sinking stream is not very likely. It can be therefore inferred that a diffuse infiltration dominates in its catchment.

There are several already existing potential sources of pollution in the catchment areas of both monitored springs such as villages, a cement factory, a warehouse for oil products, roads and railway, agricultural activities and quarries (Fig. 1). Bearing in mind a karst nature of the aquifer, the poor water quality determined by chemical and bacteriological analyses is therefore not a surprise. In addition to the increased content of mostly nitrates and *o*-phosphates exhibited by the Qinglongdong Spring, the Huanglongdong Spring also showed increased values of chlorides and sulfates. Bacteriological analysis indicated that the water was not suitable for direct public consumption without previous treatment to remove pollution. It is interesting that both chemical and bacteriological analyses showed that the Huanglongdong Spring had higher concentrations than the Qiaotou Ponor, which indicates additional pollution from the surface through vadose zone in the catchment area.

Conclusions

An integral survey of karst surface and underground was an important basis for assessing the potential impact of the construction of the new Kunming airport on the studied karst area. This area is a typical example of karst surface transformed into a stone forest, and yet it is unique because of the forms dictated by rock composition and permeability of the contact between rock and sediment and soil. The dolomite nodules protruding from the rock and dissecting the surface of the stone pillars give it a special stamp. The surface is slowly being denuded and the peaks of the stone forest have already been reshaped by rainwater and biocorrosion. Results showed the specific characteristics of the subsoil stone forest that indicated a high level of karstification.

The tracer test and measurements of physical, chemical and bacteriological parameters revealed the characteristics of recharge and groundwater flow within the two separated karst aquifers in the catchment of the Huanglongdong and

Qinglongdong springs. The two aquifers are highly vulnerable and water quality of the springs is endangered by various sources of pollution, predominantly from the surface. The new airport area, which is at least partly located inside the catchment areas, represents an additional threat. The planning of measures for the springs' protection should take into consideration the findings of the here presented study.

The results obtained confirm that karstological planning of infrastructure in karst regions and monitoring of major encroachments are necessary in addition to the contamination countermeasures proposed by Guo et al. (2010) for the rational development and protection of these vulnerable regions. Previous holistic karstology studies are needed for efficient planning and implementation of these activities.

Acknowledgments The research was supported under bilateral Project No. BI-CN/07-09-015 by the Slovenian Research Agency and the Ministry of Science and Technology of the People's Republic of China (code: 2004DFA02200) in the framework of Slovenia–China Cooperation in Science and Technology, 2007–2009.

References

Chen X, Gabrovšek F, Huang C et al (1998) South China Karst 1. ZRC Publishing, Ljubljana

Guo F, Jiang G (2010) Problems of Flood and Drought in a Typical Peak Cluster Depression Karst Area (SW China). Environ Earth Sci, Advances in Research in Karst Media, Part 1:107–113

Guo F, Yuan DX, Qin ZJ (2010) Groundwater contamination in karst areas of Southwestern China and recommended countermeasures. Acta Carsol 39/2:389–399

Jiang Y, Yuan D, Zhang C, Zhang G, He R (2008) Impact of land use change on groundwater quality in a typical karst watershed of southwest China. Hydrogeol J 16(4):727–735

Jiang Y, Wue Y, Groves C, Yuan D, Kambesis P (2009) Natural and anthropogenic factors affecting the groundwater quality in the Nandong karst underground river system in Yunan, China. J Contam Hydrol 109:49–61

Knez M, Kogovšek J, Kranjc A, Liu H, Petrič M, Slabe T (2009) The Shuilian cave in the upper region of the Chang River (Karst of NW Yunnan, China). Acta Carsol 38/1:97–106

Knez M, Liu H, Slabe T (2010a) High Mountain Karren in Northwestern Yunnan, China. Acta Carsol 39/1:103–114

Knez M, Liu H, Slabe T (eds) (2010b) South China Karst 2. ZRC Publishing, Ljubljana

Kogovšek J (2010) Characteristics of Underground Water Flow at Different Water Levels in Tianshengan Karst Area, Yunnan, China. Acta Geol Sin 84/1:206–212

Kogovšek J, Liu H (1999) Water tracing test in Tianshengan region, China at low water level in November 1998. Acta Carsol 28/2:241–253

Lu Y (2006) Karst water resources and geo-ecology in typical regions of China. Environ Geol 51/5:695–699

Mulec J, Krištůfek V, Chroňáková A (2012) Comparative microbial sampling from eutrophic caves in Slovenia and Slovakia using RIDA®COUNT test kits. Int J Speleol 41/1:1–8

Shaw E (1994) Hydrology in practice. Chapman & Hall, London

Shi Z, Liu X, Liu Y, Huang Y, Peng H (2009) Catastrophic groundwater pollution in a karst environment: a study of phosphorus sludge waste liquid pollution at the Penshuidong Cave in Yunnan, China. Environ Earth Sci 59:757–763

Slabe T (1998) Rock relief of pillars in the Lunan Stone Forest. In: Chen X et al (eds) South China Karst I. ZRC Publishing, Ljubljana, pp 51–67

Slabe T (2005) Two experimental modelings of karst rock relief in plaster: subcutaneous "rock teeth" and "rock peaks" exposed to rain. Z Geomorphol 49:107–119

Slabe T, Liu H (2009) Significant subsoil rock forms. In: Ginés A, Knez M, Slabe T, Dreybrodt W (eds) Karst Rock Features–Karren Sculpturing. ZRC Publishing, Postojna-Ljubljana, pp 123–137

Greenberg AE, Clesceri LS, Eaton AD (eds) (1992) Standard methods for the examination of water and waste water, 18th edn. American Public Health Association, Washington

Toranzos GA, McFeters GA (1997) Detection of indicator microorganisms in environmental freshwaters and drinking waters. In: Hurst CJ, Knudsen GR, McInerney MJ, Stetzenbach LD, Walter MV (eds) Manual of environmental microbiology. ASM Press, Washington, pp 184–194

Zhang S, Hu H, Zhou Z, Xu K, Yan N, Li S (2005) Photosynthetic performances of transplanted *Cypripedium flavum*. Bot Bull Acad Sin 46:307–313